

UDC 612.141:004.032.26

doi: 10.32620/reks.2023.2.04

Oleh VIUNYTSKYI, Volodymyr LUKIN, Alexander TOTSKY,
Vyacheslav SHULGIN, Nadejda KOZHEMIKINA

National Aerospace University “Kharkiv Aviation Institute”, Kharkiv, Ukraine

CONTINUOUS CUFFLESS BLOOD PRESSURE MEASUREMENT USING FEED-FORWARD NEURAL NETWORK

High blood pressure (BP) or hypertension is an extremely common and dangerous condition affecting more than 18–27 % of the world population. It causes many cardiovascular diseases that kill 7.6 million people around the world per year. The most accurate way to detect hypertension is ambulatory monitoring of blood pressure lasting up to 24 h and even more. Traditional non-invasive methods for measuring BP are oscillometric and auscultatory, they use an occlusal cuff as an external pressure source. Unfortunately, cuffed BP measurement creates some inconvenience for the patient and can be inaccurate due to incorrect cuff placement. In connection with the problems caused by cuff methods, it has become necessary to develop cuffless methods for measuring blood pressure, which are based on the relationship of blood pressure with various manifestations of cardiac activity and hemodynamics, which can be recorded and measured non-invasively, without the use of a compression cuff and with simple technical means. Over the past decade, there have been many publications devoted to estimating blood pressure based on pulse wave velocity (PWV) or pulse wave transit time (PTT). However, this approach has few disadvantages. First, the measurement of BP using only PTT parameter is valid only for a given patient. Second, the linear model of the relationship between BP and PTT is valid only in a small range of BP variations. To solve this problem neural networks or linear regression models were used. The main problem with this approach is the accuracy of blood pressure measurement. This study **builds** one feed-forward neural network (FFNN) for determining systolic and diastolic blood pressure based on features extracted from electrocardiography (ECG) and photoplethysmography (PPG) signals without a cuff and calibration procedure. The **novelty** of this work is the discovery of five new key points of the PPG signal, as well as the calculation of nine new features of the ECG and PPG signals, which improve the accuracy of blood pressure measurement. The **object** of the study was the ECG and PPG signals recorded from the patient's hand. The **target** of the study was to obtain systolic and diastolic blood pressure based on an FFNN, the input arguments of which are the parameters of the ECG and PPG signals. Algorithms for estimating signal parameters based on the determination of characteristic points in the PPG signal, the position of R-peaks in the ECG signal, and parameters calculated from the relationship of time parameters and amplitude ratios of these signals are described in detail. The Pearson correlation coefficients for these parameters and BP are determined, which helps to choose the set of signal parameters valuable for BP estimation. The results obtained show that the mean absolute error \pm standard deviation for systolic and diastolic BP is equal to 1.72 ± 3.008 mmHg and 1.101 ± 1.9 mmHg, respectively; the correlation coefficients for the estimated and true BP are equal to 0.94. **Conclusions.** The model corresponds to the AAMI standard and the “A” grade in the BHS standard, which proves the high accuracy of BP assessment by the proposed approach. Comparison to other known methods was performed, which confirmed the advantages of the proposed approach.

Keywords: blood pressure; electrocardiography; photoplethysmography; neural network; feedforward neural network.

Introduction

High blood pressure (BP) or hypertension is an extremely common and dangerous condition affecting more than 18–27 % of the world's population [1]. It causes many cardiovascular diseases (CVDs), which kill 7.6 million people around the world per year [2]. At the same time, 85 % of these deaths caused by a myocardial infarction or stroke [3]. Unfortunately, a significant proportion of hypertensive patients are not even aware of their illness, while it slowly and imperceptibly damages their internal organs (brain, eyes, kidneys, blood vessels). There-

fore, hypertension is often called a silent killer [4]. Although people can measure their own BP using automated devices, evaluation by a healthcare professional is important to assess risk and related conditions [3]. To obtain an accurate diagnosis, it is necessary to correctly measure BP, which involves many factors: body position, arm position, and a properly selected cuff [5]. Failure to comply with these indications can lead to an error in BP measurement up to 10 mmHg [5], which is undesirable.

Usually, periodic measurements are used to control blood pressure. But such measurements often cannot capture sudden and rapid changes in blood pressure. The most accurate way to detect hypertension, recommended

by the American Heart Association and the American College of Cardiology, is ambulatory monitoring lasting up to 24 h [6, 7] and even more [8]. It is obvious that appropriate means are needed to perform such monitoring.

State of the Art

All existing methods for measuring BP can be divided into two groups: methods of invasive and non-invasive measurement. In invasive measurement, the pressure sensor is installed directly into an arterial vessel [9], which ensures high accuracy and continuity of measurement; however, this approach is associated with many risks.

Therefore, invasive BP measurement can be used only in cases of emergency, in a hospital setting, and under the supervision of qualified specialists. Non-invasive methods are not based on the direct measurement of intravascular BP, but on the processing and analysis of various indicators of cardiac activity and hemodynamics, indirectly related to BP; thus, they are much safer and more convenient to use.

Traditional non-invasive methods for measuring BP are oscillometric [10] and auscultatory [11], they use an occlusal cuff as an external pressure source. Unfortunately, cuffed BP measurement creates some inconvenience for the patient and can be inaccurate due to incorrect cuff placement [12]. For each pressure measurement, the cuff must be inflated and deflated, which takes some time between successive measurements [13].

Thus, it is desirable to have methods and means of measuring BP that would have the following properties:

- 1) be non-invasive for use outside the hospital;
- 2) provide the possibility of long-term measurement of blood pressure to monitor its changes over 12-24 hours;
- 3) be convenient to use in any condition, regardless of the position of the body, hand, and cuff size, described in [5];
- 4) possess high accuracy of BP measurements.

In connection with the problems caused by the use of cuff methods - the inconvenience of long-term monitoring and the inaccuracy of determining BP due to incorrect measurement - it has become necessary to develop cuffless methods for measuring blood pressure, which are based on the relationship of blood pressure with various manifestations of cardiac activity and hemodynamics (electrical, acoustic, mechanical), and their parameters, which can be recorded and measured non-invasively, without the use of a compression cuff and with fairly simple technical means (electrocardiogram, phonocardiogram, photoplethysmogram, rheogram, mechanical pulsogram, etc.). One of these explicit dependencies is the relationship between blood pressure and the velocity of the propagation of the pulse wave along the arterial

vessels [14]. Wearable devices are also actively developing, which allow long-term monitoring of blood pressure at home [15]. Various sensors allow recording signals. The work [16] considered the use of Fiber Bragg Grating (FBG) Sensors. A basic experiment was carried out, which showed the effectiveness of blood pressure measurement using the proposed sensors [17].

Over the past decade, there have been many publications devoted to estimating blood pressure based on pulse wave velocity (PWV) or pulse wave transit time (PTT) [18]. The paper [19] considers the change in the PTT parameter when using spinal anesthesia, and the results show that the PTT indicator quite accurately indicates changes in the cardiovascular system. Since this parameter reflects the changes in the cardiovascular system, it is also actively used to monitor blood pressure with additional determination of rhythm parameters [20]. Considering the features of the PPG signal, some authors [21] suggest using its additional features to determine blood pressure, which increases the accuracy of its measurements. Parameter PTT is measured as the time it takes for a pressure pulse to travel from the peak of the ECG R-wave to the peak systolic point of the PPG waveform [22]. The use of rhythm parameters in addition to the PTT parameter when determining blood pressure leads to an increase in the accuracy of its measurements [23]. All studies have used the photoplethysmogram and electrocardiogram signals to measure the PTT values and obtain blood pressure [24, 25]. However, this approach has a few disadvantages.

Problems of existing systems

First, the measurement of BP using only PTT parameter is valid only for a given patient. In this regard, it is necessary to calibrate the blood pressure monitoring system [26]. To eliminate the calibration process, various methods are proposed, for example, the use of a mathematical analysis and mathematical models of the PPG signal with the physiological parameters of the patient was proposed in the work [27]. Although this approach has shown stable results, it requires a large amount of input data on the physiological parameters of the patient. The use of alternative data sources such as Pulse Wave Signals (PWS) [28] instead of PTT did not solve the problems with the system calibration. To eliminate the calibration problem, researchers also use neural networks [29] or linear regression models [30]. These systems are flexible; one trained model can be used to determine blood pressure for different patients without repeated training procedures. However, the relationship between blood pressure and PTT parameter is formed only based on the laws of hemodynamics in elastic vessels and does not consider changes in other parameters of the circulatory system.

Second, the linear model of the relationship between BP and PTT [31] is valid only in a small range of BP variations [32] that affect the accuracy of blood pressure measurement. Other authors have shown a way to determine blood pressure based only on the ECG signal [33]. It has also been proposed to use an evaluation of blood pressure changes using vascular transit time [34] or phonocardiogram [35] instead of an ECG for pressure assessment [36, 37]. However, this also did not solve the problem of system calibration and accuracy.

For its solving, machine learning methods were also applied, using both ECG and PPG signals to calculate blood pressure [38]. Neural networks are used in a variety of tasks, such as: 1) signal [39, 40] and image processing [41]; 2) predicting dynamic processes [42, 43]. In particular, the authors in [44] demonstrated the relationship between impedance plethysmography and photoplethysmography to determine the PTT parameter. The use of the PPG intensity factor, which can track low-frequency changes in blood pressure, was proposed in [45]. The results showed that with the use of an additional parameter, the accuracy of blood pressure determination increased. In addition, new features have been proposed, such as ascending and descending slopes and peak intensity ratios to increase the accuracy of blood pressure determination [46]. An indirect relationship was determined using algorithms based on machine learning [47]. Such approaches require several data channels (e.g., ECG and PPG); however, some studies have demonstrated quite a high accuracy of blood pressure measurements using only one data channel [48, 49]. At the same time, it has been shown in [50] that the combination of ECG and PPG waves contains distinctive information that improves the accuracy of BP determination; therefore, it still seems appropriate to use two data channels to improve the accuracy of the blood pressure estimation.

Note that the use of neural networks makes it possible to employ the developed systems for determining blood pressure [51, 52] without using additional calibration procedures [53, 54]. Also, deep machine learning methods are used, which allow the determination of blood pressure without first detecting the parameters of ECG and PPG signals [55, 56]. However, this approach requires a large amount of data during training, which limits its use in the presence of a few ECG and PPG signals [57, 58]. In the presence of pathologies such as arrhythmias, it is also necessary to consider the ECG and PPG signals containing these cases in the training dataset. If such data are available, deep learning methods can accurately calculate blood pressure [59].

To improve the accuracy of the determination, one can use neural networks with memory, for example Long Short-Term Memory (LSTM) [60] or Recurrent Neural Network (RNN), which consider previous experience of calculating blood pressure. The work [61] considered the

use of four neural networks for determining systolic, diastolic, and mean arterial pressure, the architecture of these neural networks was multispherical. For prediction, three key points in the PPG signal were used: systolic rise duration, diastolic duration, and duration between systolic and diastolic peaks. The signal amplitude ratios at three characteristic points and the time ratios between these positions in the PPG signal were also used. As frequency parameters, heart rate and respiration rate were employed. The work [62] exclusively used the propagation time of a pulse wave between two points to determine the BP value through regression equations. In [63, 64], was analyzed the possibility of using regression equations for these purposes, but this approach has not allowed evaluating BP using the same regression model for different people without preliminary calibration.

In [65], measurements of 24 signs of PPG and ECG signals were used, which were then employed to determine blood pressure. However, the paper presents the calculation of four main characteristic points of the PPG signal and there are no signs associated with the ratios of amplitude values or temporal values. The work [66] proposes a new approach for predicting the arterial blood pressure (ABP) signal based only on the PPG signal.

Authors of [67] have identified 15 main features of the PPG-peak that have been used to determine blood pressure, some of which contain information about heart rate. In our previous work [63, 64], we considered two separate Feed-Forward neural networks with 6 and 7 input parameters of ECG and PPG signals to determine systolic blood pressure (SBP) and diastolic blood pressure (DBP).

Objectives and novelty

Thus, the **aim** of this work is to develop one neural network for determining systolic and diastolic blood pressure based on features extracted from ECG and PPG signals without a cuff and calibration procedure. The **novelty** of this work is the discovery of five new key points of the PPG signal, as well as the calculation of nine new features of the ECG and PPG signals, which improve the accuracy of blood pressure measurement. The **object** of the study was the ECG and PPG signals recorded from the patient's hand.

There are various methods for training neural networks, for example, using the enhanced sea predator algorithm [68], so one of the tasks of this study will be to choose the optimal training method.

1. Materials and methods of research

The main idea of continuous blood pressure assessment based on the extraction of cumulative features from

two data sources, namely ECG and PPG signals, is as follows: we use segmentation of data sources, denoising based on linear filters, and extraction of a set of features associated with BP. Then, we analyze the relationship between certain features and BP values and develop a neural network that employs the obtained features. The output parameters are estimates of systolic and diastolic blood pressure. To analyze the accuracy of these estimates, evaluated and reference (obtained using occlusion methods) blood pressure values are used to find the standard deviation between these values.

1.1. Signal recording equipment

We developed a system for single-channel recording of both ECG and PPG signals and used CardioSens BP Holter monitor recorder [69] to obtain the blood pressure reference values shown in Fig. 1 and Fig. 2. Demographic data of patients participating in the study are shown in Table 1.



Fig. 1. One-channel ECG and PPG signal recorder



Fig. 2. CardioSens ECG + BP Holter monitor recorder

The developed system for recording ECG and PPG signals has the following characteristics: a sampling rate of 1000 Hz, 12-bit resolution, and the ability to transfer data directly to a computer via Bluetooth or store these data on a memory card. The reference BP recorder “CardioSens ECG + BP Holter monitor recorder” is capable

of recording systolic and diastolic blood pressure values determined by the occlusal cuff once per minute, data are stored on a memory card or transmitted via Bluetooth. This device achieves an accuracy of ± 2 mmHg [69].

Table 1
Demographic and BP characteristics

Characteristics	Mean \pm STD or values
Height (cm)	174.5 \pm 5.42 (163-186)
Weight (g)	83 \pm 7.30 (64-102)
Per-subject SBP average (mmHg)	130.8 \pm 7.91 (111-154)
Per-subject DBP average (mmHg)	81.97 \pm 5.43 (67-95)
Age of patients	22.5 \pm 11.61 (19-52)
Total number of observations	312
Average length of observations (minutes)	40
Total number of signals' fragments	12480
Location of data collection	National Aerospace University "KhAI"
Laboratory	KhAI-Medica
Temperature in laboratory, °C	18-22
Body position	Sitting
Information about health and cardiovascular diseases of patients	N/A

The research was conducted in accordance with the protocol approved by the Academic Council and the Ethics Committee of the Kharkiv Medical Academy of Post-graduate Education, No. 24.04.21, and was performed in accordance with the principles of the Declaration of Helsinki.

1.2. Data preparation

Signal processing begins with their segmentation into intervals of one minute. This procedure is performed because the BP Holter monitor recorder is used for about one minute to inflate the cuff and measure blood pressure. Often in signal preprocessing, preliminary signal estimation and elimination of several interferences are used [70, 71]. Locally adaptive filtering methods [72] and methods of identifying the parameters of a linear object in the presence of non-Gaussian noise [73] are also actively used, which can significantly suppress interference in the considered signals. In this work, we did not conduct a preliminary assessment.

To train a neural network, 7480 segments of signals were used (60 % of the total number of 12480). The rest values have been used for verification. The values were

divided into training and test samples in such a way that the test sample contained segments of signals for people who were not employed in training. For verification, we used 5000 segments of signals (40 % of the total sample of 12480).

1.3. Signal processing

An example of recorded signals with a duration of 15 seconds is presented in Fig. 3. For noise suppression in ECG signals, we used a combination of linear filters: a low-pass filter with a cutoff frequency of 98 Hz, a high-pass filter with a cutoff frequency of 12 Hz, and a notch filter in the frequency band of 48–52 Hz.

This selection is justified by our previous studies performed for ECG signal processing in fetal electrocardiography [74, 75]. It has been shown from the results

that the use of such a set of linear filters introduces minimal distortions into the shape of the R-peak and therefore does not change the position of the QRS complex itself; however, at the same time, such processing is sufficient to suppress various kinds of interference caused by electrode movements, muscle contractions, and interference distortion [76].

For noise suppression in PPG signals, we used the following combination of linear filters: a low-pass filter with a cutoff frequency of 40 Hz and a notch filter in the frequency band of 48–52 Hz.

It has been shown that such filter characteristics for PPG signals can suppress interference caused by interference noise and eliminate high-frequency contribution interference contained in signals. The results of applying the noise reduction procedure are shown in Fig. 4, which demonstrates fragments of 15 s of ECG and PPG signals after pre-filtering.

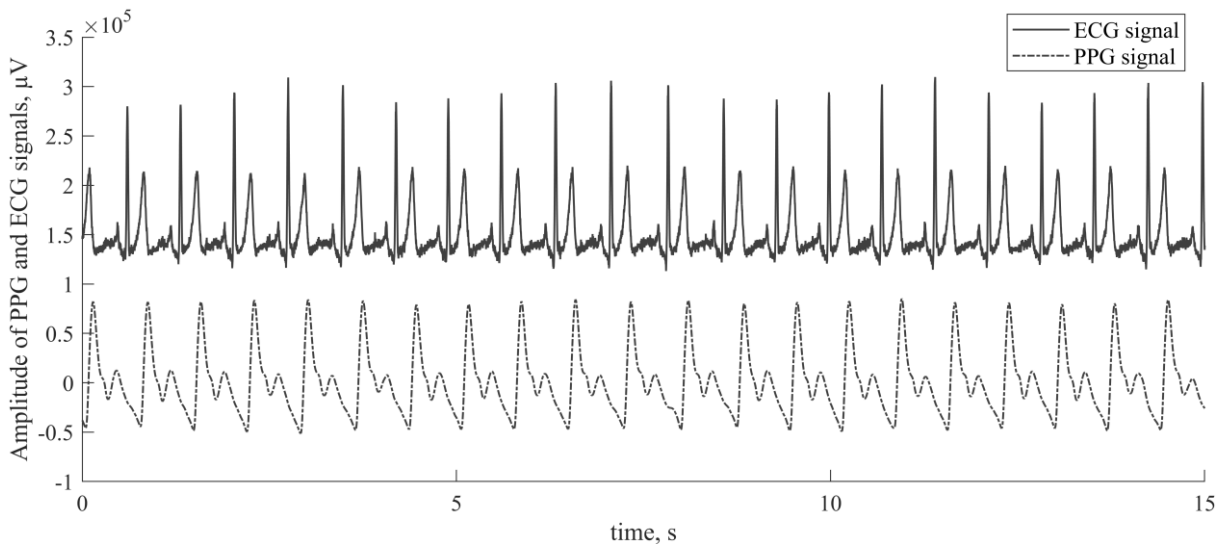


Fig. 3. An example of the obtained recordings: ECG signal (upper plot) and PPG signal (given below the ECG plot)

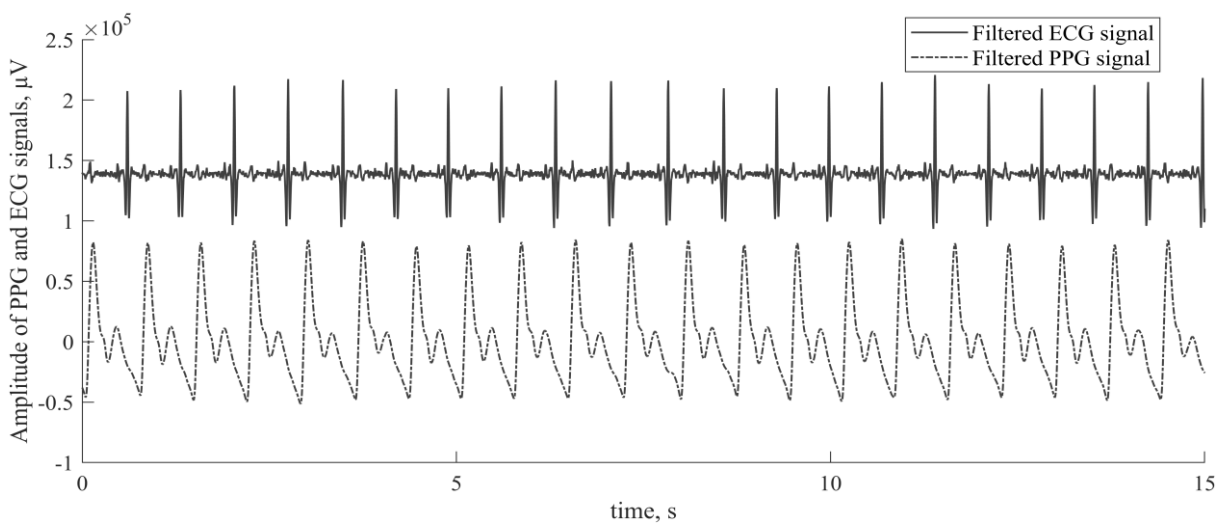


Fig. 4. ECG and PPG signals after noise reduction procedure: ECG signal (upper plot) and PPG signal (given below the ECG plot)

1.4. Feature extraction and preliminary analysis

As stated earlier, the PPT parameter is measured as the time from the R-peak point of the ECG signal to the peak systolic point of the PPG waveform, which is schematically presented in Fig. 5. To determine the positions of the R-peaks of the ECG signal and the peak systolic points of the PPG signal, a modified Pan-Tompkins algorithm was used. The threshold detector values are redefined every 10 seconds, which makes it possible to accurately determine peak positions [76]. The process of determining the positions of R-peaks in the ECG signal is shown in Fig. 6.

The PPG signal has several characteristic points that can be determined by different algorithms. In [77], the

authors used window threshold methods, but the Automatic Multiscale-based Peak Detection (AMPD) method [78, 79] demonstrated the possibility of determining the characteristic points of the PPG signal with greater stability than the threshold detection technique. In [80], the search for extrema (points of maxima and minima) of the first, second, and third derivatives of the PPG signal was applied. In our previous paper [63, 64] and in this study, we used characteristic point detection using the PPG signal and its first derivative by looking for local minima and maxima in the derivative and signal. This choice is justified by the simplicity of the implementation of this algorithm and the stable results of the search for characteristic points in the PPG signal. Fig. 7 illustrates the process of determining these positions in the PPG signal.

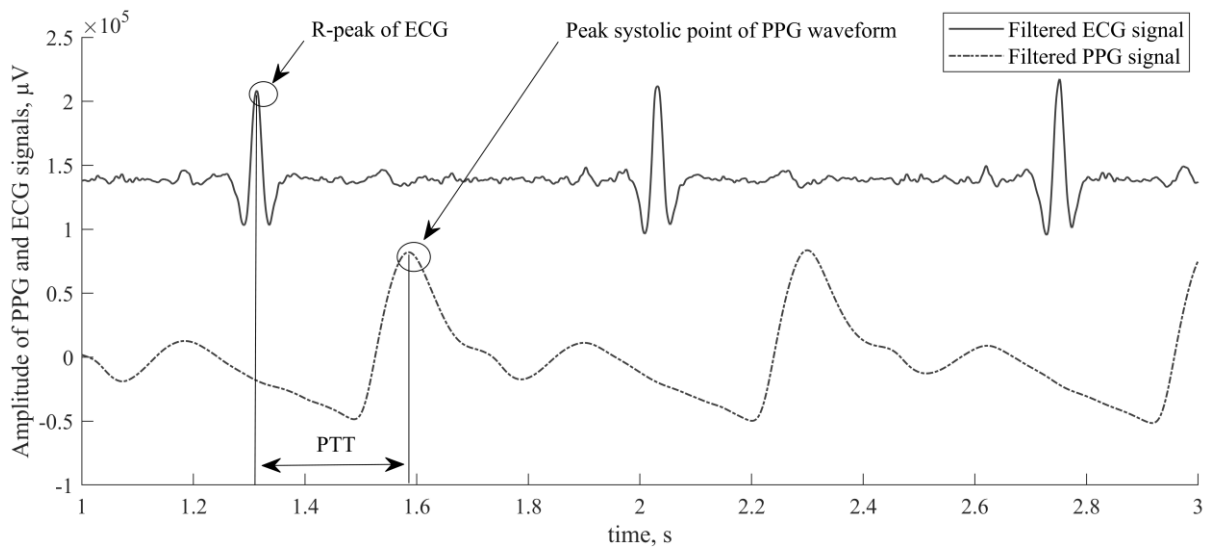


Fig. 5. Calculation of the PTT parameter as the time it takes for an impulse to travel from the R-peak point of the ECG (upper plot) to the peak systolic point of the PPG (given below the ECG plot) signals

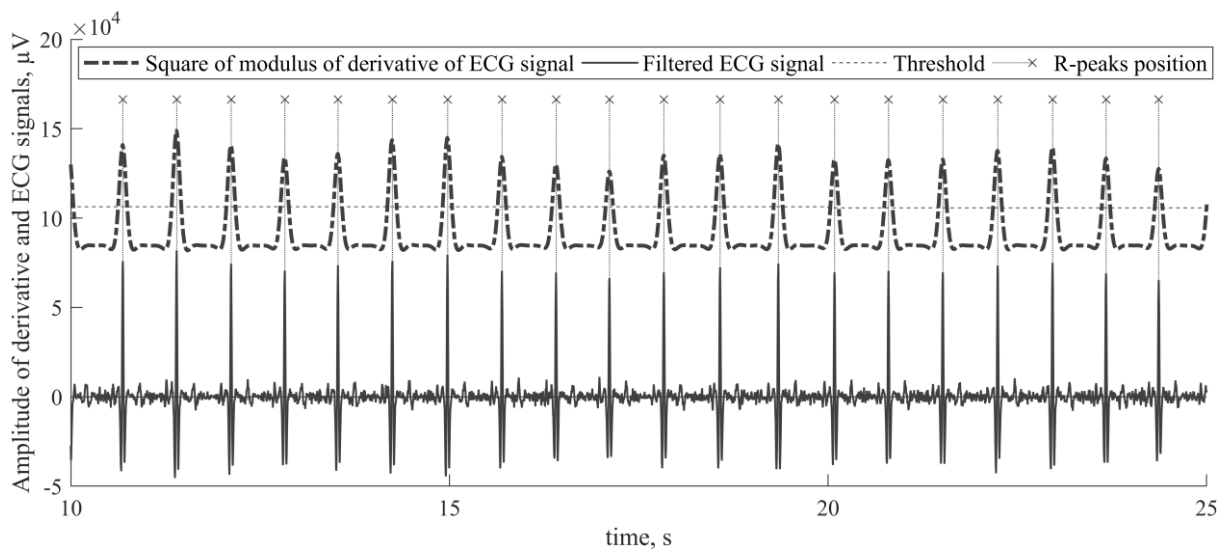


Fig. 6. R-peaks detection in ECG signal: Square of modulus of derivative of ECG signal (upper plot) and ECG signal (given below plot)

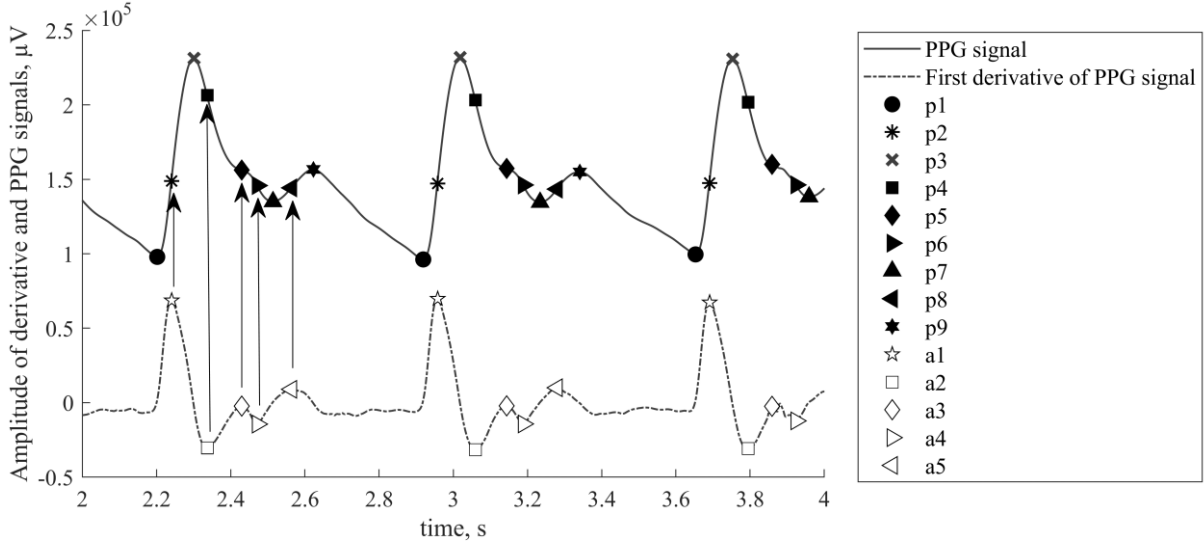


Fig. 7. PPG signal with characteristic points (upper plot) and first derivative of PPG signal with characteristic points (given below the PPG signal plot)

First, local minima and maxima are determined in the first derivative of the PPG signal, which makes it possible to detect five characteristic points of the PPG signal. Further, due to the determination of local minima and maxima of the PPG signal, the remaining characteristic points are determined, which correspond to the beginning, maximum, beginning of the second wave, and maximum of the second wave of the PPG-waveform. For example, point “p7” is defined as a local minimum of the PPG signal in the section between points “a4” and “a5”. The search procedure is described in more detail in [63, 64]. After determining all the characteristic points for the PPG signal segment lasting one min, the parameters of these signals are calculated. We consider a set of parameters that can be conditionally divided into several groups as follows: temporal and amplitude dependence of the combination of PPG and ECG signals.

1.5. Determining parameters of ECG and PPG signals

After finding all the characteristic points of the ECG (see Fig. 7) and PPG (Fig. 8) signals, it becomes possible to compute the parameters for this segment. We propose to average the calculated parameters over an interval of one signal segment lasting one minute, by sorting certain parameters for each PPG peak (for all characteristic points) from the minimum values to the maximum, then removing 10 % of the minimum and maximum (first and last) values parameters, after which the remaining ones are averaged.

This procedure avoids the contribution of falsely determined characteristic points, due to which the parameter estimates may be inaccurate. These procedures are repeated for all signals segments. To analyze the degree

of connection existing between the calculated parameters and blood pressure, we propose to evaluate the Pearson correlation coefficient between the estimated parameters and blood pressure values:

$$R = \frac{1}{n} \sum_{j=1}^n \frac{\sum_{i=1}^n (x_{j,i} - \bar{x}_j)(y_{j,i} - \bar{y}_j)}{\sqrt{\sum_{i=1}^n (x_{j,i} - \bar{x}_j)^2 \sum_{i=1}^n (y_{j,i} - \bar{y}_j)^2}}, \quad (1)$$

where n is the number of analyzed elements (number of segments); \bar{x}_j, \bar{y}_j denote average values of a considered parameter and the corresponding reference values of blood pressure; $x_{j,i}, y_{j,i}$ are reference values of an analyzed parameter and the reference values of blood pressure obtained using an occlusive tonometer.

To determine the temporal characteristics of the PPG and ECG signals, we computed the classical values of the PTT parameter from the R-peak (see Fig. 6) of the ECG signal to each characteristic point of the PPG signal (see Fig. 7) obtained earlier. The definition of this pulse transit time is schematically shown in Fig. 8.

The time series of RR intervals calculated for each R-peak of the ECG signal can be written as follows:

$$RR(i) = R(i+1) - R(i), i = 1, 2, \dots, n-1, \quad (2)$$

where $RR(i)$ is the current value of the RR-interval; $R(i+1)$ is the time of the next R-peak; $R(i)$ is the time of the current R-peak; i are indices of all R-peaks of the ECG signal, determined using the modified Pan-Tompkins algorithm; n denotes the total number of R-peaks.

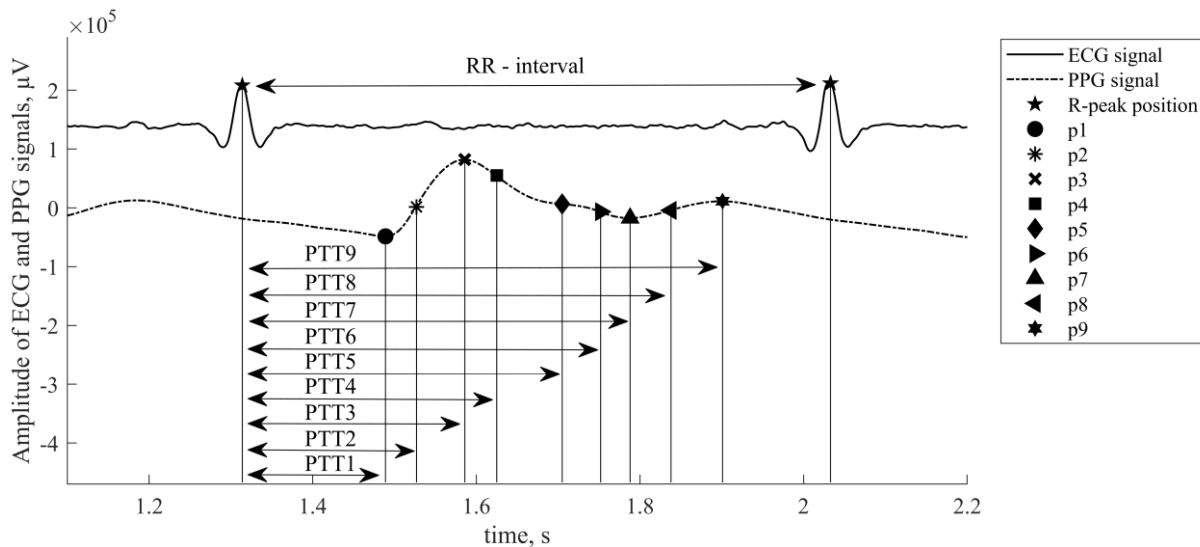


Fig. 8. Finding of pulse transit time parameters for one RR-interval (upper plot) and one PPG signal peak

Since the authors of the papers [48, 49] considered the possibility of using only one data channel, we suggest first checking the possibility of computing blood pressure using only one data channel. To do this, in the PPG signal, the characteristic point p1 can be considered as the R-peak of the ECG signal, and the computation of the PTT parameters is carried out based on this characteristic point as the moment of the impulse beginning. Fig. 9 shows the calculation of the time parameters inside the PPG peak.

However, it should also be stressed that the higher the heart rate, the more heart contractions occur in one segment, which in turn also reduces the propagation time of the pulse wave. Therefore, the analysis below is devoted to finding the correlation coefficients for the product of the pulse transit time (see Fig. 9) and the duration of the RR interval.

To determine the amplitude characteristics of the waveform of the PPG signal, we use the product of the

amplitude of the PPG signal at each characteristic point by the amplitude of the PPG signal at point p3, which characterizes the maximum value of the PPG of the peak.

1.6. Neural network design

We propose to use a Feedforward neural network with one input layer of 17 neurons, three hidden layers of 64 neurons each, and one output layer of 2 neurons. The number of neurons in the input layer is equal to the number of analyzed parameters; the number of neurons in the output layer is determined by the necessity to calculate two output values: systolic and diastolic blood pressure. The number of neurons in the hidden layers was determined experimentally: by gradually increasing their number, a neural network was obtained with a minimum error in the output values. The sigmoid transfer function was used as the transfer function in the input and hidden layers:

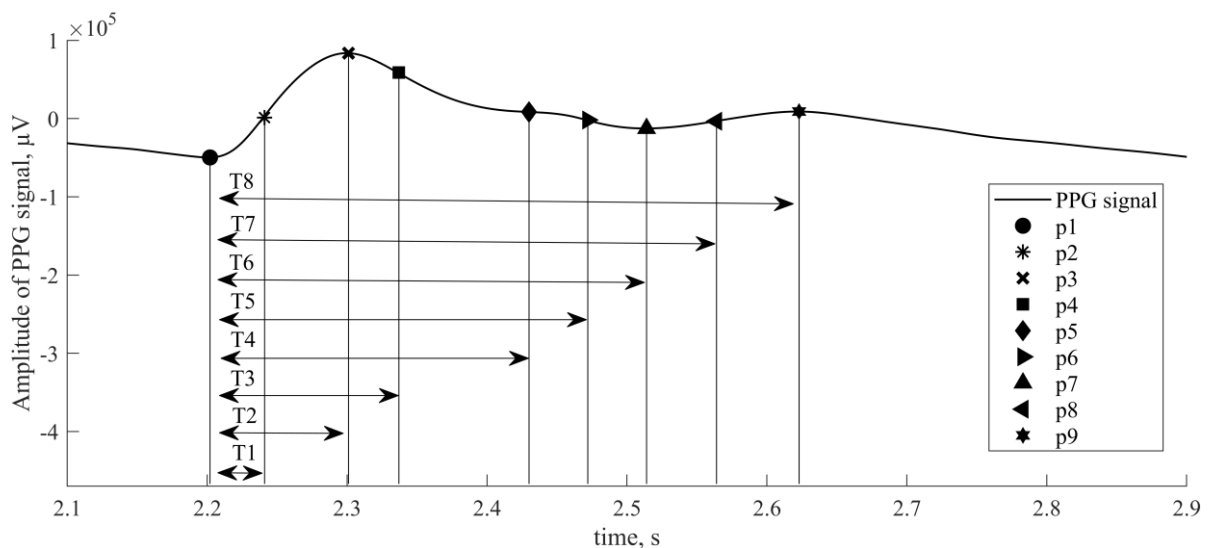


Fig. 9. Finding the pulse transit time parameters for one PPG signal peak

$$f(x) = \frac{1}{1 - e^{-x}}. \quad (3)$$

As the activation function of the output layer of the neural network, the direct (or identical) function was chosen:

$$f(x) = x. \quad (4)$$

To investigate the accuracy of blood pressure determination, we obtained an estimate of the correlation (1) between the calculated blood pressure values and the reference values, as well as additional parameters:

$$\text{mean} = \frac{\sum_{i=1}^n (x_i^{\text{EBP}} - x_i^{\text{RBP}})}{n}, \quad (5)$$

where x_i^{EBP} , x_i^{RBP} are the calculated and reference values of arterial pressure, respectively; n is the number of signal segments participating in data processing.

$$\text{MAE} = \frac{\sum_{i=1}^n |x_i^{\text{RBP}} - x_i^{\text{EBP}}|}{n}, \quad (6)$$

$$\text{SD} = \sqrt{\frac{\sum_{i=1}^n (x_i^{\text{EBP}} - x_i^{\text{RBP}} - \text{mean})^2}{n-1}}, \quad (7)$$

$$\text{LoA} = \text{mean} \pm 1.96 * \text{SD}, \quad (8)$$

$$\text{RMSE} = \sqrt{\frac{\sum_{i=1}^n (x_i^{\text{EBP}} - x_i^{\text{RBP}})^2}{n}}, \quad (9)$$

$$\text{CI} = 1.34 * \text{mean} \pm \text{LoA}. \quad (10)$$

As a training method, the Levenberg-Marquardt optimization function has been used, which updates the neuron weights and bias values. This is the fastest back-propagation algorithm. The mean squared error performance function has been used as a criterion for the accuracy of the results. It defines the mean squared error between the computed output values of the neural network and the desired reference values. Training is completed when the mean squared error reaches 0.01, in which case the network is considered trained and ready for use or testing. The weights were recalculated using the gradient descent method to achieve the learning goal.

2. Results

The results of computation (1) for the pulse transit time from the R-peak (see Fig. 6) of the ECG signal and to each characteristic point of the PPG signal (see Fig. 7), determined in all 12480 segments, are shown in Table 2.

Table 2

The correlation coefficient of the pulse transit time and reference values of systolic and diastolic blood pressure (SBP and DBP, respectively)

Parameters	Correlation coefficient	
	SBP	DBP
PTT1	-0.34	-0.17
PTT2	-0.27	-0.12
PTT3	-0.27	-0.01
PTT4	-0.03	0.18
PTT5	-0.39	-0.23
PTT6	-0.19	-0.12
PTT7	-0.1	0.07
PTT8	-0.21	-0.06
PTT9	-0.31	-0.21

The results of computation (1) for the pulse transit time from the first characteristic point of the PPG peak and to each next point determined in all 12480 signal segments are shown in Table 3.

Table 3

The correlation coefficient of the pulse transit time and reference values of blood pressure

Parameters	Correlation coefficient	
	SBP	DBP
T1	-0.18	-0.09
T2	-0.15	-0.003
T3	-0.01	-0.05
T4	-0.26	-0.3
T5	-0.2	-0.25
T6	-0.02	0.16
T7	-0.17	-0.03
T8	-0.27	-0.23

As can be seen from the results in Table 3, the modulus values of the correlation coefficients have decreased compared to the corresponding values in Table 2. As described in [50], the combined use of parameters extracted from ECG and PPG signals gives greater accuracy in determining blood pressure, as evidenced by the calculated coefficients. However, it should be noted that the relationship between the parameters and blood pressure values remained the same: with an increase in the transit time of the pulse wave, the values of arterial pressure tend to decrease, and with a decrease in the transit time, they

tend to increase. It can be concluded that high blood pressure accelerates the propagation of the pulse wave along the arterial vessel.

The results of computation (1) for the time ratio between the first characteristic point of the PPG signal and each subsequent one (see Fig. 9) to the time of the RR interval are shown in Table 4.

Table 4
The correlation coefficient of the product of the pulse transit time and the duration of the RR-interval and the reference values of blood pressure

Parameters	Correlation coefficient	
	SBP	DBP
T1/RR	0.35	-0.47
T2/RR	0.49	-0.57
T3/RR	0.43	-0.29
T4/RR	0.53	-0.67
T5/RR	0.57	-0.58
T6/RR	0.62	-0.54
T7/RR	0.61	-0.55
T8/RR	0.67	-0.51

According to Table 4, the product of the pulse transit time and the RR interval time has the highest degree of correlation with blood pressure values. It has been demonstrated in [81, 82] that the parameters of heart rate variability and current heart rate can be used to measure stroke volume and cardiac output, which also depend on blood pressure.

The results of computation of the values (1) for the ratio of the amplitude of the PPG signal at the time point p3 to the amplitude of the PPG signal at each other characteristic point of the PPG signal (see Fig. 9) are given in Table 5.

Based on the results of assessing the degree of correlation of the proposed parameters (see Tables 2-5) with SBP and DBP, we have decided to use the values of the parameters PTT1, PTT5, PTT9, T4, T1/RR-interval, T2/RR-interval, T3/RR-interval, T4/RR-interval, T5/RR-interval, T6/RR-interval, T7/RR-interval,

T8/RR-interval, as well as amplitude ratios PPG(p4)/PPG(p3), PPG(p5)/PPG(p3), PPG(p6)/PPG(p3), PPG(p7)/PPG(p3), PPG(p8)/PPG(p3) as features for determining blood pressure, since the modulo values of these parameters have larger correlation values with blood pressure values than other parameters.

Table 5
The correlation coefficients of the product of the value of the PPG signal at each key point by the value of the PPG signal at point p3 and reference values of blood pressure

Parameters	Correlation coefficient	
	SBP	DBP
PPG(p2)/PPG(p3)	-0.28	-0.14
PPG(p4)/PPG(p3)	-0.36	0.41
PPG(p5)/PPG(p3)	-0.31	0.48
PPG(p6)/PPG(p3)	-0.31	0.52
PPG(p7)/PPG(p3)	-0.3	0.45
PPG(p8)/PPG(p3)	-0.16	0.34

The parameters were selected in such a way that their modular values of the correlation coefficient for systolic or diastolic blood pressure were greater than 0.3.

Thus, 17 parameters will be further employed to measure BP. A neural network was obtained, which is shown in Fig. 10. As input arguments, the parameters listed in Tables 2-5 are used, and as the desired values at the output of the neural network, the blood pressure values obtained using the occlusive tonometer are employed. To achieve the results of the training procedure, the neural network took 27953 training epochs.

Here P denotes the input parameters that are used to calculate blood pressure; W1...5 define the weights or coefficients by which the output values of the previous layer are multiplied; b1...5 define the offset of the inputs; the sign Σ denotes the adder; a1...5 are the layer output parameters.

Fig. 11 illustrates the accuracy of BP determination by the proposed NN for finding systolic blood pressure.

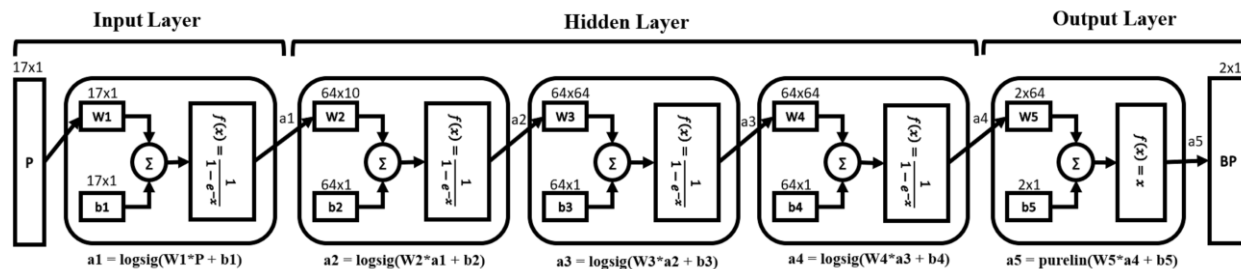


Fig. 10. Structure of the designed FFNN with some details

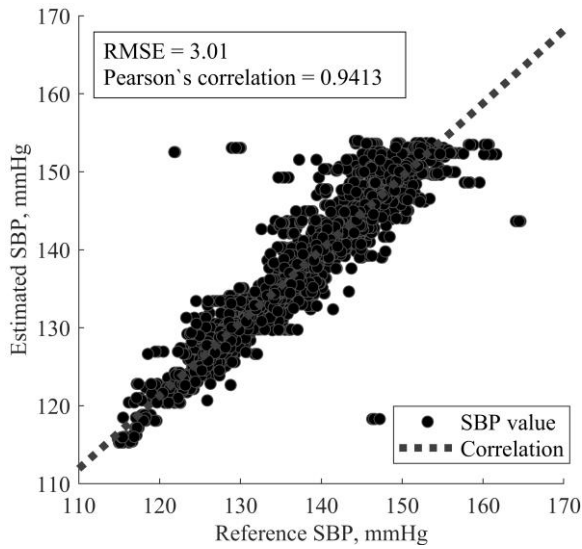


Fig. 11. Estimation of the accuracy of determining the BP for the proposed neural network model: SBP correlation coefficient plot

As can be seen from the results, the Pearson correlation coefficients are 0.9413 and the RMSEs are 3.01 mmHg for systolic BP. Fig. 12 illustrates the accuracy of BP determination by the proposed neural network for finding diastolic blood pressure. As can be seen from the results, the Pearson correlation coefficients are 0.9434 and the RMSEs are 1.89 mmHg diastolic BP.

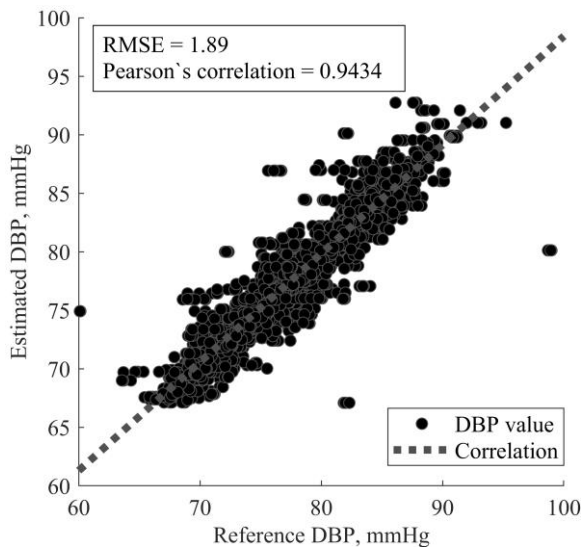


Fig. 12. Estimation of the accuracy of determining the BP for the proposed neural network model: DBP correlation coefficient plot

These results show the high accuracy of blood pressure estimation using the proposed neural network. It can also be seen that blood pressure estimates calculated using the developed NN have a linear relationship with

blood pressure estimates obtained using an occlusive tonometer. The calculated values are close to the regression line. Fig. 13-14 shows the average values and values of the difference between the calculated values of blood pressure and the reference values obtained from the occlusive tonometer using the Bland-Altman plot for systolic and diastolic BP respectively. The results show that 95 % of the calculated data fall within the confidence interval, and the mean error is close to zero, which indicates a high degree of accuracy in calculating BP values.

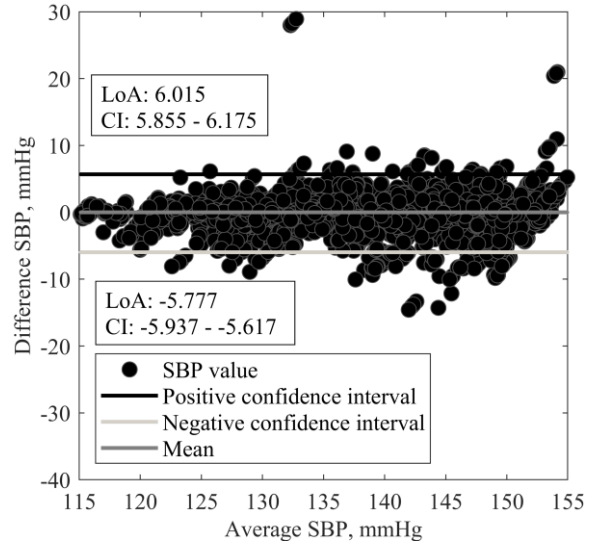


Fig. 13. Estimation of the accuracy of determining the BP of the proposed neural network model: SBP Bland-Altman plot (mean = 0.1193)

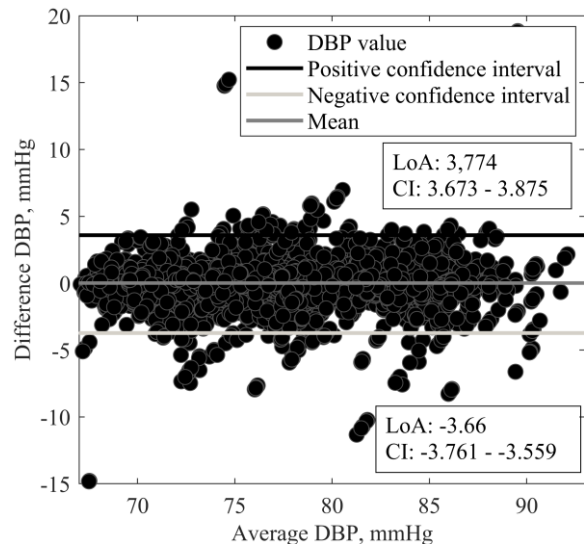


Fig. 14. Estimation of the accuracy of determining the BP of the proposed neural network model: DBP Bland-Altman plot (mean = 0.057)

Fig. 15-16 also shows error distribution histograms, from which most of the errors are in the range of

5 mmHg, which confirms the high accuracy of BP calculation by the proposed NN plot for systolic and diastolic BP respectively. A comparative analysis of the results with data obtained from other researchers is given in Table 6.

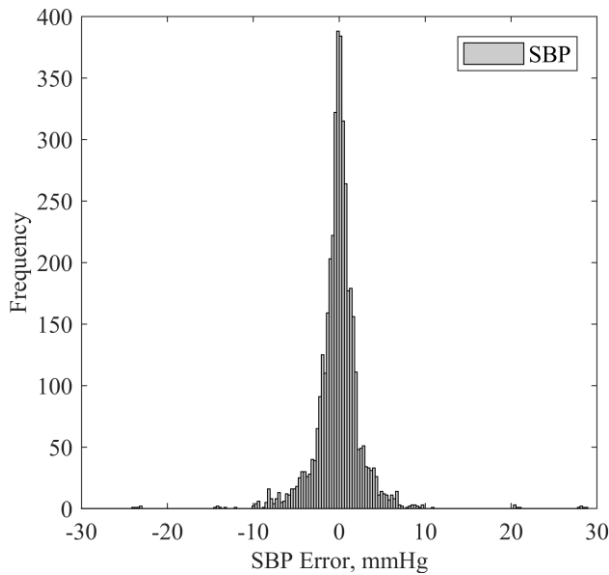


Fig. 15. SBP error distribution histogram

To evaluate the results obtained, the accuracy of the developed NN can also be carried out according to international standards AAMI and BHS. According to the AAMI standard, 85 subjects must be used for the test, and 312 were used in our study. ME values must be lower than 5 mmHg - 0.1193 mmHg and 0.057 mmHg were obtained for systolic and diastolic BP, respectively. Standard deviation (7) should be within 8 mmHg; in our case, deviations equal to 3.008 mmHg and 1.8998 mmHg were obtained for systolic and diastolic blood pressure, respectively. These results show that the accuracy of the designed system satisfies the AAMI standard. The cumulative percentage of errors in SBP is 93.72, 99.28, and 99.48 %, respectively, and for DBP - 97.64, 99.53, and 99.8 %, respectively, which is higher than the BHS class A standard of 60, 85 and 95 % of cumulative percentage.

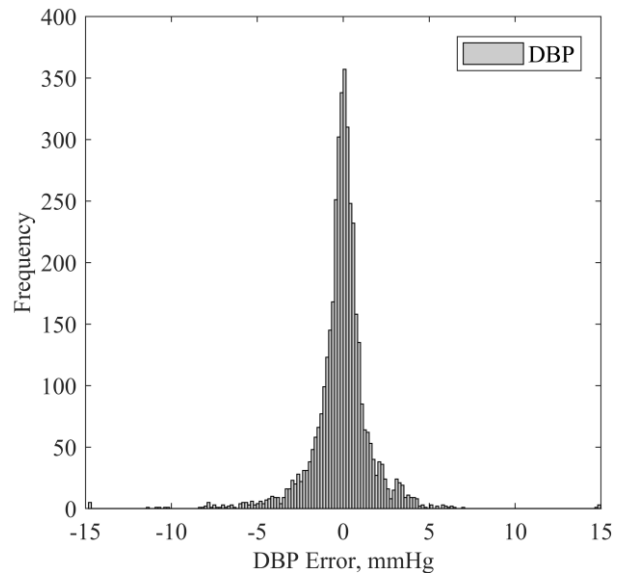


Fig. 16. DBP error distribution histogram

3. Discussion

The presented results show that the designed FFNN can provide a high accuracy of BP estimation in the statistical sense. Meanwhile, it follows from Figures 13 and 14 that certain random outliers might be present in the data (although they happen to rather small probability). We have not rejected them in the process of estimation of the mean and standard deviation. Meanwhile, we plan to conduct a special study to understand the reasons for such estimates. We hope that this can further improve the accuracy of our approach. Also, in definition (2), the value of the position of the next R-peak is used to calculate the RR-interval, which is still unknown for the current PPG-peak, due to which the calculation may be difficult in real time. It is difficult to fairly compare our results concerning estimation accuracy to the corresponding results in the papers [29-33] because of the different numbers of records analyzed, use of different databases. Meanwhile, MAE±SD in these papers varies from 4.04±5.81 mmHg in [49] till 11.17±10.09 mmHg in [30] for the systolic BP and from 2.29±3.39 mmHg in [49] till 5.35±6.14 mmHg in [30]

Table 6

Comparative analysis with other works

Work	Subjects	Number of models	SBP (MAE±SD), mmHg	DBP (MAE±SD), mmHg
Rong et al., [29]	11546 samples	2	5.59±7.25	3.36±4.48
Kachuee et al., [30]	942 subjects	2	11.17±10.09	5.35±6.14
Gaurav et al., [31]	3000 subjects	2	4.47±6.85	3.21±4.72
Li et al.,[53]		1	6.726±14.505	2.51±6.442
Malayeri et al.,[52]	21334 samples	1	4.04±5.81	2.29±3.39
Early our work [64]	5046 samples	2	3.59±4.37	2.92±3.7
This work	12480 samples	1	1.72±3.008	1.101±1.9

for the diastolic BP. Analysis shows that we have provided smaller MAE and SD values in all cases. All calculations were performed not on open databases, but on a private database, which is why it is also impossible to say precisely about the stability of this method, it is necessary to conduct experimental studies on open databases in the future for the possibility of comparing the results with other works.

Conclusions

In this paper, we propose a new method for continuous non-invasive and cuffless measurement (monitoring) of blood pressure based on the parameters of two signals: ECG and PPG. Features of signal segments are extracted by detecting R-peaks of the ECG by the modified Pan-Tompkins algorithm, as well as by detecting characteristic points of the PPG signal. Next, the informative parameters were calculated. Correlation analysis of these parameters made it possible to identify features having the maximum modular value of the correlation coefficients with the reference values of blood pressure obtained using the standard occlusive method. For all signal segments, features were extracted and averaged, which were later used to train and test the neural network. The designed neural network is Feedforward neural network. The total number of neurons in this network is 211, which is almost 4 times less compared to our previous works [60-61]. In addition, unlike the previous work, we developed a neural network to measure both systolic and diastolic blood pressure simultaneously. At the same time, the results of testing the developed neural network demonstrated the following performance characteristics: $MAE \pm SD = 1.72 \pm 3.008$ mmHg and 1.101 ± 1.9 mmHg for systolic and diastolic BP, respectively; $RMSE = 3.01$ mmHg and 1.896 mmHg for systolic and diastolic BP, respectively; Pearson's correlation coefficients between calculated and reference BP values are 94 % and 94 % for systolic and diastolic BP, respectively. 93.72 and 97.64 % of the obtained BP estimates using the developed neural network have a deviation within ± 5 mmHg. These indicators correspond to the AAMI standard and the "A" grade in the BHS standard, which proves the high accuracy of BP assessment by the proposed approach. Comparison to other known methods was performed, which confirmed the advantages of the proposed approach.

Our further research will include the following steps: 1) application of non-linear filters to suppress interference in ECG and PPG signals, such as wavelet-based or Kalman filters; 2) application of convolutional neural networks to determine blood pressure, which should increase the accuracy of the proposed method of determining blood pressure; 3) use of interpolation and

normalization methods to the PPG signal to eliminate errors due to differences in the amplitude parameters of the signal from person to person.

Contribution of authors: conceptualization – **Oleh Viunytskyi, Alexander Totsky and Vyacheslav Shulgin**; methodology – **Oleh Viunytskyi and Volodymyr Lukin**; software – **Oleh Viunytskyi**; validation – **Oleh Viunytskyi, Nadejda Kozhemiakina and Volodymyr Lukin**; formal analysis – **Oleh Viunytskyi, Alexander Totsky and Volodymyr Lukin**; investigation – **Volodymyr Lukin, Oleh Viunytskyi, Alexander Totsky and Vyacheslav Shulgin**; resources – **Oleh Viunytskyi and Vyacheslav Shulgin**; data curation – **Alexander Totsky**; visualization – **Oleh Viunytskyi**; supervision – **Volodymyr Lukin, Alexander Totsky and Oleh Viunytskyi**; project administration – **Volodymyr Lukin**.

References

1. *Hypertension: Information, Facts and Statistics. Disabled World*, 2023. Available at: <https://www.disabled-world.com/health/cardiovascular/hypertension> (accessed 2 March 2023).
2. Arima, H., Barzi, F. & Chalmers, J. Mortality patterns in hypertension. *Journal of Hypertension*, 2011, vol. 29, iss. 1, pp. 3-7. DOI: 10.1097/01.hjh.0000410246.59221.b1.
3. *Raised Blood Pressure*, 2020. Available at: http://www.who.int/gho/ncd/risk_factors/en/ (accessed 20 Sep. 2020).
4. *WHO. A global brief on Hypertension, Silent killer, global public health crisis*, 2013. Available at: <https://apps.who.int/iris/rest/bitstreams/195800/retrieve> (accessed 20 May 2023).
5. Viera, A. Screening for Hypertension and Lowering Blood Pressure for Prevention of Cardiovascular Disease Events. *Medical Clinics of North America*, 2017, vol. 101, iss. 4, pp. 701-712. DOI: 10.1016/j.mcna.2017.03.003.
6. Whelton, P., Carey, R., Aronow, W., Casey Jr, D., Collins, K., Himmelfarb, C., DePalma, S., Gidding, S., Jamerson, K., Jones, D., MacLaughlin, E., Muntner, P., Ovbigele, B., Smith Jr, S., Spencer, C., Stafford, R., Taler, S., Thomas, R., Williams Sr, K., Williamson, J. & Wright Jr, J. T. ACC/AHA/AAPA/ABC/ACPM/AGS/APhA/ASH/ASPC/NMA/PCNA Guideline for the Prevention, Detection, Evaluation, and Management of High Blood Pressure in Adults: A Report of the American College of Cardiology/American Heart Association Task Force on Clinical Practice Guidelines. *Hypertension*, 2018, vol. 71, iss. 6, pp. e13-e115. DOI: 10.1161/HYP.0000000000000065.

7. Siu, A. Screening for high blood pressure in adults: U.S. Preventive Services Task Force recommendation statement. *Annals of Internal Medicine*, 2015, vol. 163, iss. 10, pp. 778-786. DOI:10.7326/m15-2223.
8. Bakris, G., Ali, W. & Parati, G. ACC/AHA versus ESC/ESH on hypertension guidelines: JACC guideline comparison. *Journal of the American College of Cardiology*, 2019, vol. 73, iss. 23, pp. 3018-3026. DOI: 10.1016/j.jacc.2019.03.507.
9. Lam, S., Liu, H., Jian, Z., Settels, J. &Bohringer, C. Intraoperative Invasive Blood Pressure Monitoring and the Potential Pitfalls of Invasively Measured Systolic Blood Pressure. *Cureus Journal of Medical Science*, 2021, vol. 13, iss. 8, article no. e17610. DOI: 10.7759/cureus.17610.
10. Geddes, L., Voelz, M. & Combs, C. Characterization of the oscillometric method for measuring indirect blood pressure. *Annals of Biomedical Engineering*, 1982, vol. 10, iss. 6, pp. 271-280. DOI: 10.1007/BF02367308.
11. Geddes, L., Hoff, H. & Badger, A. Introduction of the auscultatory method of measuring blood pressure—including a translation of Korotkoff's original paper. *Cardiovascular research center bulletin*, 1966, vol. 5, iss. 2, pp. 57-74. PMID: 5341624. Available at: <https://pubmed.ncbi.nlm.nih.gov/5341624/> (accessed 28 April 2023).
12. George, J. &MacDonald, T. Home blood pressure monitoring. *European Cardiology Review*, 2015, vol. 10, iss. 2, pp. 95-100. DOI: 10.15420/ecr.2015.10.2.95.
13. Campbell, N., Chockalingam, A. &Fodor, J., McKay, D. Accurate, reproducible measurement of blood pressure. *Canadian Medical Association Journal*, 1990, vol. 143, iss. 1, pp. 19-22. PMID: 2192791. Available at: <https://pubmed.ncbi.nlm.nih.gov/2192791/> (accessed 3 May 2023).
14. More, W. &Barbé, K. Influence of the cuff deflation mode on oscillometric blood pressure measurements. *In Proceedings of the IEEE international workshop*, Bari, Italy, 30-31 May 2011, pp. 652-656. DOI: 10.1109/MeMeA.2011.5966650.
15. Thomas, S., Nathan, V. & Zong, C. BioWatch: a noninvasive wrist-based blood pressure monitor that incorporates training techniques for posture and subject variability. *IEEE Journal of Biomedical and Health Informatics*, 2014, vol. 20, iss. 5, pp. 1291-1300. DOI: 10.1109/JBHI.2015.2458779.
16. Miyauchi, Y., Koyama, S. & Ishizawa, H. Basic Experiment of Blood-pressure Measurement which Uses FBG Sensors. *In Proceedings of the Instrumentation and measurement technology conference*, Minneapolis, MN, USA, 6-9 May 2013, pp. 1767-1770. DOI: 10.1109/I2MTC.2013.6555718.
17. Katsuragawa, Y. & Ishizawa, H. Non-invasive blood pressure measurement by pulse wave analysis using FBG sensor. *In Proceedings of the Instrumentation and measurement technology conference*, Pisa, Italy, 11-14 May 2015, pp. 511-515. DOI: 10.1109/I2MTC.2015.7151320
18. Ahlstrom, C., Johansson, A. & Uhlin, F. Noninvasive investigation of blood pressure changes using the pulse wave transit time: a novel approach in the monitoring of hemodialysis patients. *Journal of Artificial Organs*, 2005, vol. 8, iss. 3, pp. 192-197. DOI: 10.1007/s10047-005-0301-4.
19. Sharwood-Smith, G., Bruce, J. & Drummond, G. Assessment of pulse transit time to indicate cardiovascular changes during obstetric spinal anaesthesia. *British Journal of Anaesthesia*, 2005, vol. 96, iss. 1, pp. 100-105. DOI: 10.1093/bja/aei266.
20. Cattivelli, F. & Garudadri, H. Noninvasive Cuffless Estimation of Blood Pressure from Pulse Arrival Time and Heart Rate with Adaptive Calibration. *In Proceedings of the IEEE BSN Sixth international workshop*, Berkeley, CA, USA, 03-05 June 2009, pp. 114-119. DOI: 10.1109/BSN.2009.35.
21. He, X., Goubran, R. & Liu, X. Secondary peak detection of PPG signal for continuous cuffless arterial blood pressure measurement. *IEEE Transactions on Instrumentation and Measurement*, 2014, vol. 63, iss. 6, pp. 1431-1439. DOI: 10.1109/TIM.2014.2299524.
22. Ahmad, S., Chen, S. & Soueidan, K. Electrocardiogram-assisted blood pressure estimation. *IEEE Transactions on Biomedical Engineering*, 2012, vol. 59, iss. 3, pp. 608-618. DOI: 10.1109/TBME.2011.2180019.
23. Wang, R., Jia, W. & Mao, Z. Cuff-Free Blood Pressure Estimation Using Pulse Transit Time and Heart Rate. *In Proceedings of the 12th international conference on signal processing*, Hangzhou, China, 19-23 October 2014, pp. 115-118. DOI: 10.1109/ICOSP.2014.7014980.
24. Tanveer, S. & Hasan, K. Cuffless blood pressure estimation from electrocardiogram and photoplethysmogram using waveform based ANN-LSTM network. *Biomedical Signal Processing and Control*, 2019, vol. 51, pp. 382-392. DOI: 10.1016/j.bspc.2019.02.028.
25. Kumar, S. & Ayub, S. Estimation of Blood Pressure by Using Electrocardiogram (ECG) and Photo-Plethysmogram (PPG). *In Proceedings of the 5th international conference on communication systems and network technologies*, Gwalior, India, 4-6 April 2015, pp. 521-524. DOI: 10.1109/CSNT.2015.99.
26. Yan, Y. & Zhang, Y. A Novel Calibration Method for Noninvasive Blood Pressure Measurement Using Pulse Transit Time. *In Proceedings of the 4th IEEE-EMBS International Summer School and Symposium on Medical Devices and Biosensors St Catharine's College*, Cambridge, UK, 19-22 August 2007, pp. 22-24. DOI: 10.1109/ISSMDBS.2007.4338283.

27. Rundo, F., Ortis, A., Battiato, S. & Conoci, S. Advanced Bio-Inspired System for Noninvasive Cuff-Less Blood Pressure Estimation from Physiological Signal Analysis. *Computation*, 2018, vol. 6, iss. 3, article no. 46. DOI: 10.3390/computation6030046.
28. Liu, Z., Liu, J., Wen, B., He, Q., Li, Y. & Miao, F. Cuffless Blood Pressure Estimation Using Pressure Pulse Wave Signals. *Sensors*, 2018, vol. 18, iss. 12, article no. 4227. DOI: 10.3390/s18124227.
29. Rong, M. & Li, K. A multi-type features fusion neural network for blood pressure prediction based on photoplethysmography. *Biomedical Signal Processing and Control*, 2021, vol. 68, article no. 102772. DOI: 10.1016/j.bspc.2021.102772.
30. Kachuee, M., Kiani, M., Mohammadzade, H. & Shabany, M. Cuff-Less Blood Pressure Estimation Algorithms for Continuous Health-Care Monitoring. *IEEE Transactions on Biomedical Engineering*, 2017, vol. 64, pp. 859-869. DOI: 10.1109/TBME.2016.2580904.
31. Gaurav, A., Maheedhar, M., Tiwari, V. & Narayanan, R. Cuff-less PPG based continuous blood pressure monitoring: a smartphone based approach. In *Proceedings of the 38th Annual International Conference of the IEEE Engineering in Medicine and Biology Society*, 16-20 August 2016, Orlando, FL, USA, pp. 607-610. DOI: 10.1109/EMBC.2016.7590775.
32. Zhang, Q., Chen, X., Zhen, F. & Xia, S. Cuffless blood pressure measurement using pulse arrival time and Kalman filter. *Journal of Micromechanics and Microengineering*, 2017, vol. 27, iss. 2, article no. 024002. DOI: 10.1088/1361-6439/27/2/024002.
33. Simjanoska, M., Gjoreski, M. & Gams, M. Non-invasive blood pressure estimation from ECG using machine learning techniques. *Sensors*, 2018, vol. 18, iss. 4, article no. 1160. DOI: 10.3390/s18041160.
34. Foo, J., Lim, C. & Wang, P. Evaluation of blood pressure changes using vascular transit time. *Physiological Measurement*, 2006, vol. 27, iss. 8, pp. 685-694. DOI: 10.1088/0967-3334/27/8/003.
35. Peng, R., Yan, W. & Zhang, N. Cuffless and continuous blood pressure estimation from the heart sound signals. *Sensors*, 2015, vol. 15, iss. 9, pp. 23653-23666. DOI: 10.3390/s150923653.
36. Chandrasekaran, V., Dantu, R. & Jonnada, S. Cuffless differential blood pressure estimation using smart phones. *IEEE Transactions on Biomedical Engineering*, 2013, vol. 60, iss. 4, pp. 1080-1089. DOI: 10.1109/TBME.2012.2211078.
37. Shukla, S., Kakwani, K. & Patra, A. Noninvasive cuffless blood pressure measurement by vascular transit time. In *Proceedings of the 28th international conference on VLSI Design*, Bangalore, India, January 2015, pp. 535-540. DOI: 10.1109/VLSID.2015.96.
38. Wu, C., Chuang, C. & Chen, Y. A new estimate technology of non-invasive continuous blood pressure measurement based on electrocardiograph. *Advances in Mechanical Engineering*, 2016, vol. 8, iss. 6, pp. 1-8. DOI: 10.1177/1687814016653689.
39. Hazra, S., Ema, R., Galib, S., Kabir, S. & Adnan, N. Emotion recognition of human speech using deep learning method and MFCC features. *Radioelektronni i komp'uterni sistemi. Radioelectronic and computer systems*, 2022, vol. 4, pp. 161-172. DOI: 10.32620/reks.2022.4.13.
40. Martínez-Sellés, M. & Marina-Breyse, M. Current and Future Use of Artificial Intelligence in Electrocardiography. *Journal of Cardiovascular Development and Disease*, 2023, vol. 10, iss. 4, article no. 175. DOI: 10.3390/jcdd10040175.
41. Moskalenko, V. & Moskalenko, A. Neural network based image classifier resilient to destructive perturbation influences – architecture and training method. *Radioelektronni i komp'uterni sistemi – Radioelectronic and computer systems*, 2022, vol. 3, pp. 95-109. DOI: 10.32620/reks.2022.3.07.
42. Krivtsov, S., Menailov, I., Bazilevych, K. & Chumachenko, D. Predictive model of COVID-19 epidemic process based on neural network. *Radioelektronni i komp'uterni sistemi – Radioelectronic and computer systems*, 2022, vol. 4, pp. 7-18. DOI: 10.32620/reks.2022.4.01.
43. Malte, S. & Hagemeyer, A. Developing Feedforward Neural Networks as Benchmark for Load Forecasting: Methodology Presentation and Application to Hospital Heat Load Forecasting. *Energies*, 2023, vol. 16, iss. 4, article no. 2026. DOI: 10.3390/en16042026.
44. Huynh, T., Jafari, R. & Chung, W. Noninvasive cuffless blood pressure estimation using pulse transit time and impedance plethysmography. *IEEE Transactions on Biomedical Engineering*, 2019, vol. 66, pp. 967-976. DOI: 10.1109/tbme.2018.2865751.
45. Ding, X., Zhang, Y., Liu, J., Dai, W. & Tsang, H. Continuous cuffless blood pressure estimation using pulse transit time and photoplethysmogram intensity ratio. *IEEE Transactions on Biomedical Engineering*, 2016, vol. 66, iss. 4, pp. 964-972. DOI: 10.1109/TBME.2015.2480679.
46. Lin, W. New photoplethysmogram indicators for improving cuffless and continuous blood pressure estimation accuracy. *Physiological Measurement*, 2018, vol. 39, iss. 2, article no. 025005. DOI: 10.1088/1361-6579/aaa454.
47. Al-Abed, M., Al-Bashir, A., Al-Rawashdeh, A., Alex, R., Zhang, R., Watenpugh, D. & Behbehani, K. Estimation of cerebral blood flow velocity during breath-hold challenge using artificial neural networks. *Computers in Biology and Medicine*, 2019, vol. 115, article no. 103508. DOI: 10.1016/j.compbiomed.2019.103508.

48. Soh, D., Ng, E., Jahmunah, V., Oh, S., Tan, R. & Acharya, U. Automated diagnostic tool for hypertension using convolutional neural network. *Computers in Biology and Medicine*, 2020, vol. 126, article no. 103999. DOI: 10.1016/j.combiomed.2020.103999.
49. Wu, C., Chuang, C., Chen, Y. & Chen, S. A new estimate technology of non-invasive continuous blood pressure measurement based on electrocardiograph. *Advances in Mechanical Engineering*, 2016, vol. 8, iss. 6. DOI:10.1177/1687814016653689.
50. Esmaelpoor, J., Moradi, M. & Kadkhodamohammadi, A. Cuffless blood pressure estimation methods: Physiological model parameters versus machine-learned features. *Physiological Measurement*, 2021, vol. 42, article no. 035006. DOI: 10.1088/1361-6579/abeae8.
51. Hengbing, J., Lili, Z., Dequn, H. & Qianjin, F. Continuous Blood Pressure Estimation Based on Multi-Scale Feature Extraction by the Neural Network with Multi-Task Learning. *Frontiers in Neuroscience*, 2022, vol. 16, article no. 883693. DOI: 10.3389/fnins.2022.883693.
52. Malayeri, A. & Khodabakhshi, M. Concatenated convolutional neural network model for cuffless blood pressure estimation using fuzzy recurrence properties of photoplethysmogram signals. *Scientific reports*, 2022, vol. 12, article no. 6633. DOI: 10.1038/s41598-022-10244-6.
53. Li, Y., Harfiya, L., Purwandari, K. & Lin, Y. Real-Time Cuffless Continuous Blood Pressure Estimation Using Deep Learning Model. *Sensors*, 2020, vol. 20, article no. 5606. DOI: 10.3390/s20195606.
54. González, S., Hsieh, W. & Chen, T. A benchmark for machine-learning based non-invasive blood pressure estimation using photoplethysmogram. *Scientific Data*, 2023, vol. 10, article no. 149. DOI: 10.1038/s41597-023-02020-6.
55. Pilz, N., Patzak, A. and Bothe, T. Continuous cuffless and non-invasive measurement of arterial blood pressure-concepts and future perspectives. *Blood Pressure*, 2022, vol. 31, iss. 1, pp. 254-269. DOI: 10.1080/08037051.2022.2128716.
56. Athaya, T. & Choi, S. Real-Time Cuffless Continuous Blood Pressure Estimation Using 1D Squeeze U-Net Model: A Progress toward mHealth. *Biosensors*, 2022, vol. 12, article no. 655. DOI: 10.3390/bios12080655.
57. Zhou, K., Yin, Z., Peng, Y. & Zeng, Z. Methods for Continuous Blood Pressure Estimation Using Temporal Convolutional Neural Networks and Ensemble Empirical Mode Decomposition. *Electronics*, 2022, vol. 11, article no. 1378. DOI: 10.3390/electronics11091378.
58. Harfiya, L., Chang, C. & Li, Y. Continuous Blood Pressure Estimation Using Exclusively Photoplethysmography by LSTM-Based Signal-to-Signal Translation. *Sensors*, 2021, vol. 21, article no. 2952. DOI: 10.3390/s21092952.
59. ZengDing, L., Bin, Z., Ye, L., Min, T. & Fen, M. Continuous Blood Pressure Estimation from Electrocardiogram and Photoplethysmogram During Arrhythmias. *Frontiers in Physiology*, 2020, vol. 11, article no. 575407. DOI: 10.3389/fphys.2020.575407.
60. Che, X., Li, M., Kang, W., Lai, F. & Wang, J. Continuous Blood Pressure Estimation from Two-Channel PPG Parameters by XGBoost. In *Proceedings of the 2019 IEEE International Conference on Robotics and Biomimetics (ROBIO)*, Dali, China, 06-08 December 2019, pp. 2707-2712. DOI: 10.1109/ROBIO49542.2019.8961600.
61. Tarifi, B., Fainman, A., Pantanowitz, A. & Rubin, D. A Machine Learning Approach to the Non-Invasive Estimation of Continuous Blood Pressure Using Photoplethysmography. *Applied Sciences*, 2023, vol. 13, article no. 3955. DOI: 10.3390/app13063955.
62. Hangsik, S. A novel method for non-invasive blood pressure estimation based on continuous pulse transit time: An observational study. *Psychophysiology*, 2023, vol. 60, iss. 2, article no. e14173. DOI: 10.1111/psyp.14173.
63. Viunytskyi, O., Shulgin, V., Sharonov, V. & Totsky, A. Non-invasive Cuff-less Measurement of Blood Pressure Based on Machine Learning. In *Proceedings of the IEEE 15th International Conference on Advanced Trends in Radioelectronics, Telecommunications and Computer Engineering*, Lviv-Slavske, Ukraine, 25-29 February 2020, pp. 203-206. DOI: 10.1109/TCSET49122.2020.235423.
64. Viunytskyi, O., Shulgin, V., Totsky, A. & Egiazarian, K. Human Blood Pressure Measurement Using Machine Learning Strategy. *Telecommunications and Radio Engineering*, 2022, vol. 81, iss. 3, pp. 1-21. DOI: 10.1615/TelecomRadEng.2022037783.
65. Wong, M., Hei, H., Lim, S. & Ng, E. Applied machine learning for blood pressure estimation using a small, real-world electrocardiogram and photoplethysmogram dataset. *Mathematical Biosciences and Engineering*, 2023, vol. 20, iss. 1, pp. 975-997. DOI: 10.3934/mbe.2023045.
66. Brophy, E., Vos, M., Boylan, G. & Ward, T. Estimation of Continuous Blood Pressure from PPG via a Federated Learning Approach. *Sensors*, 2021, vol. 21, article no. 6311. DOI: 10.3390/s21186311.
67. Harfiya, L., Chang, C. & Li, Y. Continuous Blood Pressure Estimation Using Exclusively Photoplethysmography by LSTM-Based Signal-to-Signal Translation. *Sensors*, 2021, vol. 21, article no. 2952. DOI: 10.3390/s21092952.
68. Jinzhong, Z. & Xu, Y. Training Feedforward Neural Networks Using an Enhanced Marine Predators

Algorithm. *Processes*, 2023, vol. 11, iss. 3, article no. 924. DOI: 10.3390/pr11030924.

69. XAI-MEDICA, *Equipment's catalog*, 2023. Available at: <https://xai-medica.com/en/equipments.html> (accessed 3 March 2023)

70. Ghosh, R., Phadikar, S., Deb, N., Sinha, N., Das, P. & Ghaderpour, E. Automatic Eyeblink and Muscular Artifact Detection and Removal from EEG Signals Using k-Nearest Neighbor Classifier and Long Short-Term Memory Networks. *IEEE Sensors Journal*, 2023, vol. 23, iss. 5, pp. 5422-5436. DOI: 10.1109/JSEN.2023.3237383.

71. Abramov, S., Abramova, V., Krivenko, S. & Lukin, V. Analiz i prohnozuvannya efektyvnosti fil'tratsiyi odnovymirnykh syhnaliv na osnovi dyskretnoho kosynusnoho peretvorenniya [Analysis and prediction of filtering efficiency of one-dimensional signals based on discrete cosine transformation]. *Radioelektronni i komp'uterni sistemi – Radioelectronic and computer systems*, 2019, vol. 3, pp. 19-29. DOI: 10.32620/reks.2019.3.02. (In Russian).

72. Tulyakova, N. & Trofymchuk, O. Lokal'no-adaptivna fil'tratsiya nestatsionarnoho shumu v tryvalykh elektrokardiohrafichnykh syhnalakh [Locally adaptive filter of non-stationary noise in long-term electrocardiographic signals]. *Radioelektronni i komp'uterni sistemi – Radioelectronic and computer systems*, 2020, vol. 4, pp. 16-33. DOI: 10.32620/reks.2020.4.02 (In Russian).

73. Rudenko, O. & Bezsonov, O. Adaptive identification under the maximum correntropy criterion with variable center. *Radioelektronni i komp'uterni sistemi – Radioelectronic and computer systems*, 2022, vol. 1, pp. 216-228. DOI: 10.32620/reks.2022.1.17.

74. Viunytskyi, O. & Shulgin, V. Fetal ECG and heart rhythm analyzing using BabyCard. *In Proceedings of the 2017 Signal Processing Symposium*, Jachranka, Poland, 12-14 September 2017, pp. 1-4. DOI: 10.1109/SPS.2017.8053640.

75. Viunytskyi, O. & Shulgin, V. Signal processing techniques for fetal electrocardiogram extraction and analysis. *In Proceedings of the IEEE 37th International*

Conference on Electronics and Nanotechnology, Kyiv, Ukraine, 18-20 April 2017, pp. 325-328. DOI: 10.1109/ELNANO.2017.7939772.

76. Shulgin, V. & Viunytskyi, O. Spatio-temporal signal processing for fetus and mother state monitoring during pregnancy. *In Proceedings of the IEEE 9th International Conference on Dependable Systems, Services and Technologies*, Kyiv, Ukraine, 24-27 May 2018, pp. 677-680. DOI: 10.1109/DESSERT.2018.8409210.

77. Jacobson, A. Auto-threshold peak detection in physiological signals. *In Proceedings of the 2001 Conference Proceedings of the 23rd Annual International Conference of the IEEE Engineering in Medicine and Biology Society*, Istanbul, Turkey, 25-28 October 2001, vol. 3, pp. 2194-2195. DOI: 10.1109/IEMBS.2001.1017206.

78. Scholkmann, F., Boss, J. & Wolf, M. An efficient algorithm for automatic peak detection in noisy periodic and quasi-periodic signals. *Algorithms*, 2012, vol. 5, iss. 4, pp. 588-603. DOI: 10.3390/a5040588.

79. Navid, H., Mahdi, A. & Hoda, M. Blood Pressure Estimation Using Photoplethysmogram Signal and Its Morphological Features. *IEEE Sensors Journal*, 2019, vol. 20, iss. 8, pp. 4300-4310. DOI: 10.1109/JSEN.2019.2961411.

80. Clémentine, A., João, J., Jérôme, Z., Martin, P., Guillaume, B., Pascal, F. & Mathieu, L. Blood pressure monitoring during anesthesia induction using PPG morphology features and machine learning. *PLOS One*, 2023, vol. 18, iss. 2, article no. e0279419. DOI: 10.1371/journal.pone.0279419.

81. Poon, C. & Zhang, Y. Cuff-less and noninvasive measurements of arterial blood pressure by pulse transit time. *In Proceedings of the 2005 IEEE Engineering in Medicine and Biology 27th Annual Conference*, Shanghai, China, 17-18 January 2006, pp. 5877-5880. DOI: 10.1109/IEMBS.2005.1615827.

82. Jadooei, A., Zaderykhin, O. & Shulgin, V. Adaptive algorithm for continuous monitoring of blood pressure using a pulse transit time. *In Proceedings of the Electronics and Nanotechnology (ELNANO)*, Kyiv, Ukraine, 16-19 April 2013, pp. 297-301. DOI: 10.1109/ELNANO.2013.6552042.

Received 25.03.2023, Accepted 20.05.2023

БЕЗПЕРЕРВНЕ ВИМІРЮВАННЯ АРТЕРІАЛЬНОГО ТИСКУ БЕЗ МАНЖЕТИ ЗА ДОПОМОГОЮ ПРЯМОЇ НЕЙРОННОЇ МЕРЕЖІ

Олег В'юницький, Володимир Лукін, Олександр Тоцький,
Вячеслав Шулгін, Надія Кожемякіна

Високий кров'яний тиск (АТ) або гіпертонія є надзвичайно поширеним і небезпечним станом, яким страждає понад 18–27 % населення світу. Він є причиною багатьох серцево-судинних захворювань, які щорічно вбивають 7,6 мільйонів людей у всьому світі. Найточнішим способом виявлення артеріальної гіпертензії є амбулаторне спостереження за артеріальним тиском тривалістю до 24 годин і навіть більше. Традиційними неінвазивними методами вимірювання АТ є осцилометричний і аускультативний, вони використовують оклюзійну манжету як джерело зовнішнього тиску. На жаль, вимірювання АТ за допомогою манжети створює певні

незручності для пацієнта і може бути неточним через неправильне розміщення манжети. У зв'язку з проблемами використання манжетних методів виникла необхідність у розробці безманжетних методів вимірювання артеріального тиску, які базуються на зв'язку артеріального тиску з різними проявами серцевої діяльності та гемодинаміки, які можна реєструвати та вимірювати неінвазивно, без застосування компресійної манжети і простими технічними засобами. За останнє десятиліття з'явилось багато публікацій, присвячених оцінці артеріального тиску на основі швидкості пульсової хвилі (ШПХ) або часу проходження пульсової хвилі (ЧПХ). Однак цей підхід має кілька недоліків. По-перше, вимірювання АТ за допомогою лише параметра ЧПХ дійсно лише для одного пацієнта. По-друге, лінійна модель зв'язку між АТ і ЧПХ дійсна лише в невеликому діапазоні варіацій АТ. Для вирішення цієї проблеми використовувалися нейронні мережі або моделі лінійної регресії. Основною проблемою такого підходу є точність вимірювання артеріального тиску. Дане дослідження спрямоване на створенні однієї прямої нейронної мережі (ПНН) для визначення систолічного та діастолічного артеріального тиску на основі характеристик, отриманих із сигналів електрокардіографії (ЕКГ) і фотоплетизмографії (ФПГ) без використання манжети та процедури калібрування. Новизна роботи полягає у відкритті п'яти нових ключових точок сигналу ФПГ, а також обчисленні дев'яти особливостей сигналів ЕКГ і ФПГ, які підвищують точність вимірювання АТ. Об'єктом дослідження є сигнали ЕКГ та ФПГ, записані з руки пацієнта. Метою дослідження є отримання систолічного та діастолічного АТ на основі ПНН, вхідними аргументами якої є параметри сигналів ЕКГ та ФПГ. Детально описано алгоритми оцінки параметрів сигналу, засновані на визначенні характерних точок у сигналі ФПГ, положення R-піків у сигналі ЕКГ, а також параметрів, розрахованих із співвідношення часових параметрів і відношень амплітуд цих сигналів. Визначено коефіцієнти кореляції Пірсона для цих параметрів і АТ, що допомагає вибрати набір сигнальних параметрів, цінних для оцінки АТ. Отримані результати показують, що середня абсолютна похибка \pm стандартне відхилення для систолічного та діастолічного АТ дорівнює $1,72 \pm 3,008$ мм.рт.ст. та $1,101 \pm 1,9$ мм.рт.ст. відповідно; коефіцієнти кореляції для розрахункового та істинного АТ дорівнюють 0,94. Висновки. Модель відповідає стандарту ААМІ та оцінці «А» за стандартом BHS, що свідчить про високу точність оцінки АТ за запропонованим підходом. Проведено порівняння з іншими відомими методами, що підтвердило переваги запропонованого підходу.

Ключові слова: артеріальний тиск; електрокардіографія; фотоплетизмографія; нейронна мережа; нейронна мережа прямого зв'язку.

В'юницький Олег Геннадійович – асп. каф. інформаційно-комунікаційних технологій імені О. О. Зеленського, Національного аерокосмічного університету ім. М. Є. Жуковського «Харківський авіаційний інститут», Харків, Україна.

Лукін Володимир Васильович – д-р техн. наук, проф., зав. каф. інформаційно-комунікаційних технологій імені О. О. Зеленського, Національного аерокосмічного університету ім. М. Є. Жуковського «Харківський авіаційний інститут», Харків, Україна.

Тоцький Олександр Володимирович – д-р техн. наук, проф., проф. каф. інформаційно-комунікаційних технологій імені О. О. Зеленського, Національного аерокосмічного університету ім. М. Є. Жуковського «Харківський авіаційний інститут», Харків, Україна.

Шульгін Вячеслав Іванович – канд. техн. наук, проф., проф. каф. аерокосмічних радіоелектронних систем, Національного аерокосмічного університету ім. М. Є. Жуковського «Харківський авіаційний інститут», Харків, Україна.

Кожемякіна Надія Володимирівна – канд. техн. наук, старш. викл. каф. інформаційно-комунікаційних технологій імені О. О. Зеленського, Національного аерокосмічного університету ім. М. Є. Жуковського «Харківський авіаційний інститут», Харків, Україна.

Oleh Viunyskyi – PhD student of the Department of Information and Communications Technologies named after O. O. Zelensky, National Aerospace University “Kharkiv Aviation Institute”, Kharkiv, Ukraine, e-mail: o.viunyskyi@khai.edu, ORCID: 0000-0002-1806-6193, Scopus Author ID: 57194621350.

Volodymyr Lukin – Doctor of Technical Sciences, Professor, Head of the Department of Information and Communications Technologies named after O. O. Zelensky, National Aerospace University “Kharkiv Aviation Institute”, Kharkiv, Ukraine, e-mail: v.lukin@khai.edu, ORCID: 0000-0002-1443-9685.

Alexander Totsky – Doctor of Technical Sciences, Professor, Professor of the Department of Information and Communications Technologies named after O. O. Zelensky, National Aerospace University “Kharkiv Aviation Institute”, Kharkiv, Ukraine, e-mail: totskeyalexander@gmail.com.

Vyacheslav Shulgin – PhD, Professor, Professor of the Department of Aerospace Radio-Electronic Systems, National Aerospace University “Kharkiv Aviation Institute”, Kharkiv, Ukraine, e-mail: vyacheslav.shulgin@gmail.com, ORCID: 0000-0002-4128-8085.

Nadejda Kozhemiakina – PhD, Senior Lecturer of the Department of Information and Communications Technologies named after O. O. Zelensky, National Aerospace University “Kharkiv Aviation Institute”, Kharkiv, Ukraine, e-mail: n.kozhemiakina@khai.edu, ORCID: 0000-0001-8194-5847.